Luminescent properties of Eu^{3+}-doped $SmBa_3B_9O_{18}$

Ming He,[1] Z.H. Zhang,[2,a)] Y.Z. Zhu,[1] Y.G. Tang,[1] and Z. Song[1]
[1]*Department of Physics, Dalian Jiaotong University, Dalian 116028, China*
[2]*Liaoning Key Materials Laboratory for Railway, School of Materials Science and Engineering, Dalian Jiaotong University, Dalian 116028, China*

(Received 2 December 2012; accepted 19 April 2013)

Eu^{3+}-doped $SmBa_3B_9O_{18}$ luminescent materials were synthesized by high temperature solid state reactions. The structure and photoluminescence properties of $Sm_{(1-x)}Eu_xBa_3B_9O_{18}$ ($x = 0.2$, 0.4, and 0.6) were investigated by X-ray diffraction, scanning electron microscopy, energy dispersive X-ray spectroscopy, and photoluminescence spectra. The results show that doping of Eu^{3+} ions does not change the structure of $SmBa_3B_9O_{18}$. The luminescence is mainly the characteristic Eu^{3+} ion luminescence. No concentration quenching processes occur with the increment of Eu^{3+} concentration. The work implies that $SmBa_3B_9O_{18}$ is a potential host material and europium-doped $SmBa_3B_9O_{18}$ may find application in display and optical devices. © *2013 International Centre for Diffraction Data.* [doi:10.1017/S0885715613000468]

Key words: luminescent material, solid state reaction, doping, borate

I. INTRODUCTION

Luminescent materials are generally composed of a host material and a dopant, having wide applications such as cathode ray tube, color display, field emission display, optoelectronic devices, etc. (Nikl *et al.*, 2006). Rare earth ions are often used as activation centers for the abundant energy level structure. Through doping with rare earth ions, some excellent luminescent materials have been found (Pidol *et al.*, 2003). However, it is well known that low doping of rare earth ions in a compound leads to weak luminescence, while heavy doping caused "concentration quenching" of luminescence, which greatly reduced luminescence efficiency of doped rare earth ions (Dotsenko *et al.*, 2010). Thus, it is very important to explore proper host material with large doping tolerance.

Researches show that when using materials with larger anionic groups (such as BO_3, B_3O_6, PO_4, or WO_4, etc.) serving as the host material, the rare earth ions will be spaced out, and the "concentration quenching" process would scarcely occur. This phenomenon provides a direction to search for new luminescent materials. Many borate compounds show nonlinear optical properties, high transmittance in the ultraviolet (UV) region, and large birefringence (He *et al.*, 2001, 2005; Wu *et al.*, 2005; Cai *et al.*, 2007). $SmBa_3B_9O_{18}$, one of the isostructural borate compounds $REBa_3B_9O_{18}$ (RE = Sm, Gd, Tb, Lu, Y etc.) (Li *et al.*, 2005), adopts a centric space group $P6_3/m$ with unit-cell parameters $a = 7.1980$ Å and $c = 17.336$ Å, as shown in Figure 1. Three BO_3 planar groups form a planar hexagonal $[B_3O_6]^{3-}$ ring. These planar rings are parallel to each other and stack along the *c*-axis in the unit cell, with SmO_6, BaO_6, and BaO_9 polyhedra in between the hexagonal $[B_3O_6]^{3-}$ rings. Owing to the parallel planar hexagonal $[B_3O_6]^{3-}$ rings in the lattices, perhaps it might act as a potential host material for a new luminescent material through activators doping.

In this paper, we report the synthesis and luminescence properties of europium doped $SmBa_3B_9O_{18}$. The dependence of luminescence intensity on Eu^{3+} concentration shows that no concentration quenching processes occur, which implies that $SmBa_3B_9O_{18}$ is a potential host material and europium-doped $SmBa_3B_9O_{18}$ may find application in display and optical devices. This work will be helpful to explore new luminescent materials.

II. EXPERIMENTAL

Polycrystalline europium-doped $SmBa_3B_9O_{18}$ powder was synthesized from analytical reagents: Sm_2O_3, Eu_2O_3, $BaCO_3$, and H_3BO_3. The high-temperature sintering method

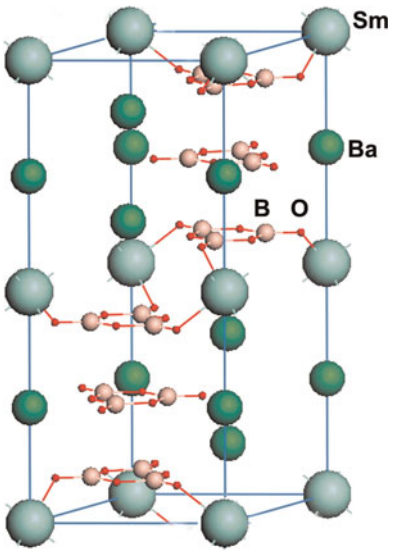

Figure 1. The crystal structure of $SmBa_3B_9O_{18}$.

a)Author to whom correspondence should be addressed. Electronic mail: zhzhang@djtu.edu.cn

was adopted to prepare the $Sm_{(1-x)}Eu_xBa_3B_9O_{18}$ ($x = 0.2$, 0.4, and 0.6) materials. Weighted raw materials were fully ground into powders and mixed uniformly in an agate mortar, and then they were placed in the box-type resistance heating furnace. The mixtures were preheated at 400 °C for 1 h to let $BaCO_3$ and H_3BO_3 decompose slowly, and then sintered at 860 °C for 3 days with intermediate grindings.

The as-prepared samples were checked by powder X-ray diffraction (XRD), energy dispersive X-ray spectroscopy (EDS), and scanning electron microscopy (SEM, SEM-JMS6360LV). The XRD patterns were measured on an X-ray Rigaku diffractometer D/Max-2400 with Cu$K\alpha$ radiation (40 kV, 140 mA) at room temperature. The emission and excitation spectra were recorded using a Hitachi-F4500-FL spectrofluorometer equipped with a xenon lamp.

III. RESULTS AND DISCUSSION

Figure 2(a) shows the simulated XRD pattern for $SmBa_3B_9O_{18}$. Figures 2(b–d) are the selected measured XRD patterns for the synthesized $Sm_{1-x}Eu_xBa_3B_9O_{18}$ materials with Eu-doping concentrations of $x = 0.2$, 0.4, and 0.6, respectively. It can be found that the XRD pattern of the sintered materials agrees with the simulated pattern and no impurity phases were detected. This implies that Eu-doping does not modify the symmetry and structure of $SmBa_3B_9O_{18}$, because Eu and Sm atoms have similar atomic radius, coordination structure, and physical–chemical properties. Continuous solid solutions are formed in the whole range ($x = 0$–0.6) for the Eu-doped $SmBa_3B_9O_{18}$ system.

The EDS results reveal only the existence of Sm, Ba, B, O, and Eu elements in the samples, as shown in Figure 3.

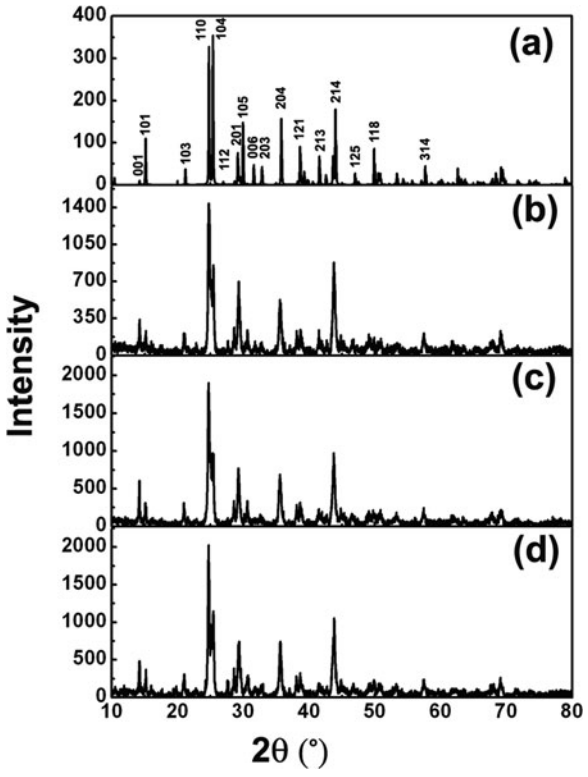

Figure 2. (a) Simulated XRD pattern of $SmBa_3B_9O_{18}$. (b) to (d) The measured XRD patterns of $Sm_{(1-x)}Eu_xBa_3B_9O_{18}$ ($x = 0.2$, 0.4, and 0.6), respectively.

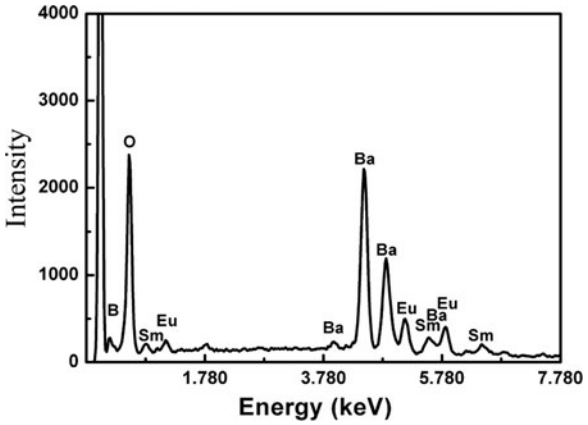

Figure 3. Typical EDS results, revealing the existence of Sm, Ba, B, O, and Eu in the samples.

Figure 4(a) shows typical SEM photographs of the synthesized $Sm_{1-x}Eu_xBa_3B_9O_{18}$ ($x = 0.6$) materials. The layered structure was observed and the prominent characteristic of $Sm_{1-x}Eu_xBa_3B_9O_{18}$ is the serious anisotropic growth. The nucleation and crystal growth were dominated by crystal bonding dynamics and external thermodynamic driving force. The growth rate along the *a*–*b*-plane is much larger than that along the *c*-axis, which can be easily understood from the periodic bond chain (PBC) theory (Hartman and Perdok, 1955; Hartman, 1956). This kind of anisotropic growth is determined by the crystal structure of $SmBa_3B_9O_{18}$ (as shown in Figure 1). The distributions of doped Eu^{3+} ions are analyzed by EDS element mapping technique, as shown in Figures 4(b–f). The element maps are acquired using Eu-$L_{\alpha1}$ (Figure 4b), Sm-$L_{\alpha1}$ (Figure 4c), Ba-$L_{\alpha1}$ (Figure 4d), B-$K_{\alpha1,2}$ (Figure 4e), and O-$K_{\alpha1}$ (Figure 4f). Eu and Sm (B and O) elements are found to have similar spatial distributions, while Ba is found to be more evenly distributed through the whole investigated region. Such spatial distributions of the compositional elements agree well with the nominal composition of the compounds, indicating that the Eu^{3+} ions were doped into $SmBa_3B_9O_{18}$ uniformly.

Figure 5(a) showed a UV excitation spectrum of Eu-doped $SmBa_3B_9O_{18}$ obtained by monitoring $^5D_0$–$^7F_1$ at 589 nm. The main broad band at 200–300 nm originates from the charge transfer (CT) transition of O–Eu^{3+} (Kodaira *et al.*, 2003). Namely, the electron delocalized from the filled 2p shell of O^{2-} to the partially filled 4f shell of Eu^{3+}. The wavelength of ~230 nm is the most effective excitation wavelength (Li *et al.*, 2008; Ding *et al.*, 2011). Figure 5(b) presents the emission spectra ($\lambda_{ex} = 230$ nm) for $Sm_{1-x}Eu_xBa_3B_9O_{18}$ ($x = 0.2$, 0.4, and 0.6), respectively. It was found that the Eu^{3+}-doped $SmBa_3B_9O_{18}$ samples presented the characteristic Eu^{3+} ion luminescence. The emission of Eu^{3+} ions in $SmBa_3B_9O_{18}$ extends from 550 to 720 nm and consists mainly of several groups of lines. Several peaks are observed at 578, 589, 594, 608, 618, 652, and 680 nm for the $Sm_{1-x}Eu_xBa_3B_9O_{18}$ series. The intensities of 589 and 608 nm peaks are the most strong. The intensity of the emission peak is increasing with the increment of Eu^{3+} ions concentration in the main and no concentration quenching processes occur. This indicates that if we continue to improve

https://doi.org/10.1017/S0885715613000468 Published online by Cambridge University Press

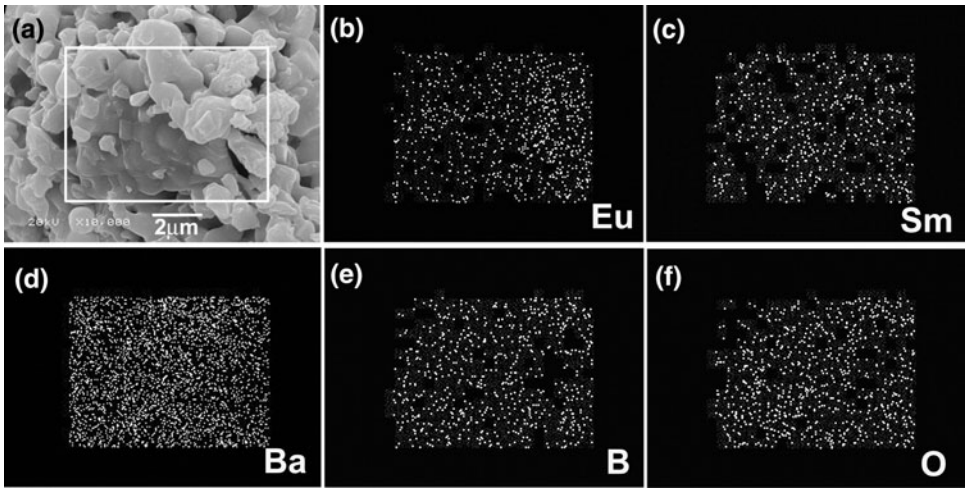

Figure 4. (a) Typical SEM images of the samples, indicating the layered structures. (b) to (d) EDS elemental mappings of Eu, Sm, Ba, B, and O elements, respectively, indicating the spatial distributions of the elements.

the Eu^{3+} doping concentration, better luminescent materials would be obtained.

The emission features of the title material are because of transitions from the excited state $^5D_0$ to the ground states ^7F_J ($J = 0$, 1, 2, 3, and 4) in the $4f^6$ configuration of Eu^{3+} ions (Aloui-Lebbou *et al.*, 2001; Dotsenko *et al.*, 2010). The main lines at around 589 nm are attributed to magnetic dipole transition of $^5D_0$–$^7F_1$ and main lines at 608 nm are because of $^5D_0$–$^7F_2$ transition (electric dipole transition). The ratios of the red emission at 608 nm to the orange one at 589 nm (abbreviated as the R/O value) are all lower than 1.00 for different Eu^{3+} contents. Therefore, the orange emission is predominant and Eu^{3+} does occupy the inversion symmetry sites in the host lattices based on the Judd–Ofelt theory (Huang *et al.*, 2009). No emission from the higher level, e.g., $^5D_{1,2}$ was detected except the transition from $^5D_0$, because the low-lying charge-transfer states skip the higher-lying ^5D_J levels during the relaxation process (Fonger and Struck, 1970). Maximum splitting numbers of transition lines for $^5D_0$–^7F_J ($J = 0$, 1, and 2) are 1 (for $J = 0$), 3 (for $J = 1$), and 5 (for $J = 2$) for each site, as a result of $2J + 1$ components for Eu^{3+} in a crystal field (Xie *et al.*, 2010). From the emission spectrum shown in Figure 5(b), one peak at 578 nm ($^5D_0$–$^7F_0$), two lines for $^5D_0$–$^7F_1$ (the third one is not obvious), and several lines for $^5D_0$–$^7F_2$ are observed. It is suggested that the Eu^{3+} ions are doped into the $SmBa_3B_9O_{18}$ matrix in one crystallographic site, which is consistent with the crystal structure of $SmBa_3B_9O_{18}$.

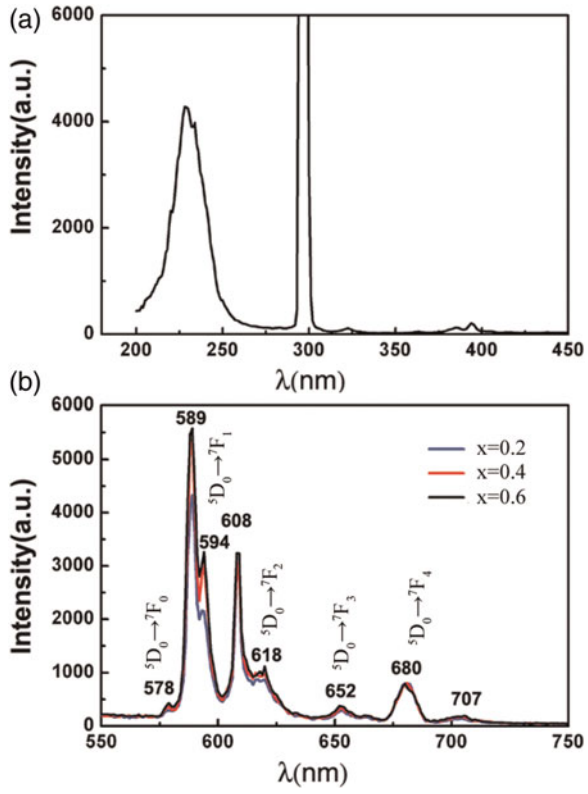

Figure 5. (a) Excitation spectra recorded in the range from 200 to 450 nm monitoring the emission at 589 nm. (b) Emission spectrum obtained in the range from 500 to 720 nm when excited at 230 nm.

IV. CONCLUSION

Europium (Eu^{3+})-doped $SmBa_3B_9O_{18}$ were synthesized by facile solid state reaction at high temperatures. XRD, SEM, and EDX measurements indicate that $Sm_{1-x}Eu_xBa_3B_9O_{18}$ formed solid solutions in the range of $x = 0$–0.6. Eu^{3+} ions doping does not change the crystal structure of the host material $SmBa_3B_9O_{18}$. $Sm_{1-x}Eu_xBa_3B_9O_{18}$ ($x = 0.2$, 0.4, and 0.6) have a strong absorption at the wavelength of ~230 nm, and show good emission performance at 589 and 608 nm under ultraviolet excitation. High luminescence efficiency is found in Eu-doped $SmBa_3B_9O_{18}$ series with the increment of Eu^{3+} concentration. The results presented here indicate that Eu-doped $SmBa_3B_9O_{18}$ may find application in phosphor.

ACKNOWLEDGEMENTS

The authors gratefully acknowledge financial support by the National Natural Science Foundation of China (Grant Nos. 50902014 and 51002017), Liaoning Province Talent Plan, LJQ2011044 and International Centre for Diffraction Data (ICDD).

https://doi.org/10.1017/S0885715613000468 Published online by Cambridge University Press

Aloui-Lebbou, O., Goutaudier, C., Kubota, S., Dujardin, C., Cohen-Adad, M., Pedrini, C., Florian, P., and Massiot, D. (**2001**). "Structural and scintillation properties of new Ce^{3+}-doped alumino-borate," Opt. Mater. **16**, 77–86.

Cai, G. M., He, M., Chen, X. L., Wang, W. Y., Lou, Y. F., Chen, H. H., and Zhao, J. T. (**2007**). "Crystal structure and luminescence properties of a novel promising phosphor $Ba_3ScB_9O_{18}$," Powder Diffr. **22**, 328–333.

Ding, H., Sun, J., Liu, W., Meng, Q., and Lu, S. (**2011**). "Effect of Sm^{3+} doping on structural and luminescent properties of $CaMoO_4:Eu^{3+}$," Chinese J. Lumin. **32**, 456–561.

Dotsenko, V. P., Berezovskaya, I. V., Efryushina, N. P., Voloshinovskii, A. S., and Stryganyuk, G. B. (**2010**). "Luminescence properties and electronic structure of Sm^{3+}-doped $YAl_3B_4O_{12}$," J. Mater. Sci. **45**, 1469–1472.

Fonger, W. H. and Struck, C. W. (**1970**). "$Eu_5^{+3}D$ resonance quenching to the charge-transfer states in Y_2O_2S, La_2O_2S, and LaOC," J. Chem. Phys. **52**, 6364–6372.

Hartman, P. (**1956**). "An approximate calculation of attachment energies for ionic crystals," Acta Crystallogr. **9**, 569–572.

Hartman, P. and Perdok, W. G. (**1955**). "On the relations between structure and morphology of crystals. III," Acta Crystallogr. **8**, 525–529.

He, M., Chen, X. L., Lan, Y. C., Li, H., and Xu, Y. P. (**2001**). "Ab initio structure determination of new compound $LiAlB_2O_5$," J. Solid State Chem. **156**, 181–184.

He, M., Chen, X. L., Okudear, H., and Simon, A. (**2005**). "$(K_{1-x}Na_x)_2Al_2B_2O_7$ with $0 \le x < 0.6$: a promising nonlinear optical crystal," Chem. Mater. **17**, 2193–2196.

Huang, J., Zhou, L., Pang, Q., Gong, F., Sun, J., and Wang, W. (**2009**). "Photoluminescence properties of a novel phosphor $CaB_2O_4:Eu^{3+}$ under NUV excitation," Luminescence **24**, 363–366.

Kodaira, C. A., Brito, H. F., and Felinto, M. C. F. C. (**2003**). "Luminescence investigation of Eu^{3+} ion in the $RE^2(WO_4)_3$ matrix (RE = La and Gd) produced using the Pechini method," J. Solid State Chem. **171**, 401–407.

Li, X. Z., Wang, C., Chen, X. L., Li, H., Jia, L. S., Wu, L., and Du, Y. X. (**2005**). "Syntheses, thermal stability and structure determination of the novel isostructural $RBa_3B_9O_{18}$ (R = Y, Pr, Nd, Sm, Eu, Gd, Tb, Dy, Ho, Er, Tm, Yb)," Inorg. Chem. **43**, 8555–8560.

Li, X., Chen, B., and Lin, H. (**2008**). "Deposition and effective red emission of Eu^{3+}-doped $Y_xTi_xO_{0.5x}$ crystal phosphor film," Chinese J. Lumin. **29**, 89–93.

Nikl, M., Pejchal, J., Mihokova, E., Mares, J. A., Ogino, H., Yoshikawa, A., Fukuda, T., Vedda, A., and Ambrosio, C. D. (**2006**). "Antisite defect-free $Lu_3(Ga_xAl_{1-x})_5O_{12}$:Pr scintillator," Appl. Phys. Lett. **88**, p141916(1–3).

Pidol, L., Kahn-Harari, A., Viana, B., Ferrand, B., Dorenbos, P., De Hass, J. T. M., Van Eijk, C. W. E., and Virey, E. (**2003**). "Scintillation properties of $Lu_2Si_2O_7:Ce^{3+}$, a fast and efficient scintillator crystal," J. Phys.: Condens. Matter **15**, 2091–2094.

Wu, L., Chen, X. L., Li, H., He, M., Xu, Y. P., and Li, X. Z. (**2005**). "Structure determination and relative properties of novel cubic borates $MM'_4(BO_3)_3$ (M = Li, M′ = Sr; M = Na, M′ = Sr, Ba)," Inorg. Chem. **44**, 6409–6414.

Xie, N., Huang, Y., Qiao, X., Shi, L., and Seo, H. (**2010**). "A red-emitting phosphor of fully concentrated Eu^{3+}-based molybdenum borate $Eu_2MoB_2O_9$," Mater. Lett. **64**, 1000–1002.

https://doi.org/10.1017/S0885715613000468 Published online by Cambridge University Press